Computational homogenization of masonry using the finite-volume direct averaging micromechanics theory

Rafael Leandro C. Silva, Severino P. C. Marques

Center of Technology, Federal University of Alagoas
Campus A. C. Simoes, Maceió, 57072-900, Alagoas, Brazil.
rafael.costa@ifal.edu.br, smarques@ctec.ufal.br

Abstract. This paper presents a study focused on determining effective elastic properties of masonry made up of bricks and mortar joints arranged in periodic arrays. The brick and mortar are treated as linear elastic materials, with a bond pattern consisting of stacked bond and running bond. The overall effective elastic moduli are evaluated by a computational unit cell-based micromechanical procedure. The formulation employs a discretization of the masonry unit cell which is examined using the finite-volume direct averaging micromechanics theory (FVDAM). The homogenization approaches are carried out considering plane stress (PS) and generalized plane strain (GPS) states, as well as a tridimensional version of the FVDAM theory (3D-FVDAM). The results provided by these three conditions of analysis (PS, GPS, 3D-FVDAM) are compared in order to verify their limitations and applicability in the elastic homogenization of periodic masonry with different geometric features.

Keywords: masonry, micromechanics, homogenization, FVDAM.

1 Introduction

Masonry is an important construction material with heterogeneous microstructure composed of two phases (mortar and bricks) usually arranged in periodic arrays. The heterogeneous and anisotropic behaviors exhibited by the masonry, as well as the physical nonlinearity of the constituent phases, make its theoretical modeling a very hard task. Nevertheless, an accurate knowledge of the masonry mechanical behavior is crucial for designing and retrofitting the masonry structural systems. In the last decades, a large number of experimental and theoretical studies have been developed aiming at understanding the behavior of masonry. The heterogeneous characteristics of the masonry become its effective behavior more sophisticated than that exhibited by the traditional homogeneous systems. The effective response of masonry is strongly dependent on the physical properties, volume fractions and spatial distribution of the bricks and mortar joints. In the context of theoretical analysis, the micromechanical homogenization models play a very important role [1]. Among these procedures, there are the analytical models based on the mean-field micromechanics [2-4] and computational homogenization approaches with formulations developed using numerical tools, such as finite-element method [2, 5], finite-volume theory [6] and mechanics of structure gene [7].

This paper presents a study on the effective elastic properties of masonry made up of bricks and mortar joints arranged in periodic arrays. The brick and mortar are treated as linear elastic materials, with a bond pattern consisting of stack bond and running bond. The overall effective elastic moduli are evaluated by a computational unit cell-based micromechanical procedure developed using the finite-volume direct averaging micromechanics theory (FVDAM). The homogenization approaches are carried out considering plane stress (PS) and generalized plane strain (GPS) states, as well as a tridimensional version of the FVDAM theory (3D-FVDAM). The results provided by these three conditions of analysis (PS, GPS, 3D-FVDAM) are compared in order to verify their

limitations and applicability in the elastic homogenization of periodic masonry with different geometric features.

2 Considerations on elastic homogenization of periodic heterogeneous material

In usual masonry wall, the bricks are arranged in periodic patterns. Two important topologies, known as stack bond and running bond, are shown in Figure 1. Due to the masonry system periodicity, the homogenization approach can be developed using a repeating unit cell (RUC), which characterizes the periodic heterogeneity. Figure 1 also shows RUC examples for the two different brick arrays. For a periodic brick arrangement, there are several options of RUC configurations to be used in the homogenization procedure.

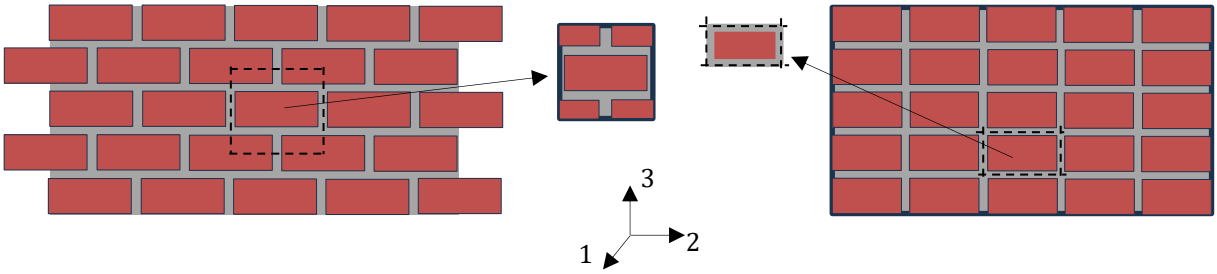

(a) (b)

Figure 1. Arrangements of bricks in masonry: a) running bond; b) stack bond.

Consider a very large masonry wall, with volume V and boundary surface S, subjected to a uniform displacement boundary condition $\boldsymbol{u}^0(\boldsymbol{x}) = \boldsymbol{\varepsilon}^0\boldsymbol{x}$ prescribed at superficial points $\boldsymbol{x} \in S$. Here, $\boldsymbol{\varepsilon}^0$ is a strain matrix with constant components ε_{ij}^0 $(i,j = 1,2,3)$. Under this boundary condition, the displacement field within the RUC can be expressed, using a two-scale representation, in the form

$$\boldsymbol{u}(\boldsymbol{y}) = \boldsymbol{\varepsilon}^0\boldsymbol{x} + \boldsymbol{u}'(\boldsymbol{y}), \tag{1}$$

where $\boldsymbol{y}$ denotes the local coordinates of the RUC scale, the first term on the right side represents the macroscopic contribution and $\boldsymbol{u}'$ is the fluctuating displacement vector. Due to the homogeneity of the boundary conditions and periodicity of the masonry, $\boldsymbol{u}'(\boldsymbol{y})$ is a periodic function over the RUC domain Ω. The subdomains of Ω occupied by the brick and joint materials are denoted by Ω_b and Ω_m, respectively. The strain field in the RUC is given by

$$\boldsymbol{\varepsilon}(\boldsymbol{y}) = \boldsymbol{\varepsilon}^0 + \boldsymbol{\varepsilon}'(\boldsymbol{y}), \tag{2}$$

where $\boldsymbol{\varepsilon}'$ is the strain matrix corresponding to the fluctuating displacement $\boldsymbol{u}'$. The average strain $\bar{\boldsymbol{\varepsilon}}$ and average stress $\bar{\boldsymbol{\sigma}}$ on the RUC domain Ω are defined by the following relations

$$\bar{\boldsymbol{\varepsilon}} = \frac{1}{|\Omega|}\int_{\Omega} \boldsymbol{\varepsilon}(\boldsymbol{y})d\Omega \qquad \text{and} \qquad \bar{\boldsymbol{\sigma}} = \frac{1}{|\Omega|}\int_{\Omega} \boldsymbol{\sigma}(\boldsymbol{y})d\Omega. \tag{3}$$

Now, suppose that the RUC domain is divided into N homogenous subdomains $\Omega^{(k)}$ $(k = 1, \cdots N)$. Similarly, the average strain and average stress on the subdomain $\Omega^{(k)}$ are defined by

$$\bar{\boldsymbol{\varepsilon}}^{(k)} = \frac{1}{|\Omega|^{(k)}}\int_{\Omega^{(k)}} \boldsymbol{\varepsilon}(\boldsymbol{y})d\Omega^{(k)} \qquad \text{and} \qquad \bar{\boldsymbol{\sigma}}^{(k)} = \frac{1}{|\Omega|^{(k)}}\int_{\Omega^{(k)}} \boldsymbol{\sigma}(\boldsymbol{y})d\Omega^{(k)}. \tag{4}$$

If $\boldsymbol{C}^{(k)}$ is the stiffness matrix of the phase (brick or joint) occupying the k-th subdomain, the corresponding constitutive relation is written as

$$\bar{\boldsymbol{\sigma}}^{(k)} = \boldsymbol{C}^{(k)}\bar{\boldsymbol{\varepsilon}}^{(k)}. \tag{5}$$

Using (3) and (4), the following expressions can be easily derived

$$\bar{\boldsymbol{\varepsilon}} = \sum_{k=1}^{N} c^{(k)}\, \bar{\boldsymbol{\varepsilon}}^{(k)} \qquad \text{and} \qquad \bar{\boldsymbol{\sigma}} = \sum_{k=1}^{N} c^{(k)}\, \bar{\boldsymbol{\sigma}}^{(k)}, \tag{6}$$

where $c^{(k)} = |\Omega|^{(k)}/|\Omega|$.

In accordance with the known average strain theorem, the average strain on the entire RUC $\bar{\boldsymbol{\varepsilon}}$ is equal to the macroscopic strain $\boldsymbol{\varepsilon}^0$. Then, the average fluctuating strain on the RUC domain is null. This can be explained by the periodicity of the field $\boldsymbol{\varepsilon}'(\boldsymbol{y})$ on Ω. Using micromechanical considerations, it is concluded that the average strain $\bar{\boldsymbol{\varepsilon}}^{(k)}$ can be related to the macroscopic strain $\bar{\boldsymbol{\varepsilon}}$ by

$$\bar{\boldsymbol{\varepsilon}}^{(k)} = \boldsymbol{A}^{(k)}\bar{\boldsymbol{\varepsilon}}, \tag{7}$$

where $\boldsymbol{A}^{(k)}$ is the strain concentration matrix of the subdomain $\Omega^{(k)}$. In a similar way, the relation between the average stress $\bar{\boldsymbol{\sigma}}^{(k)}$ and the average stress on the entire RUC ($\bar{\boldsymbol{\sigma}}$) is given as

$$\bar{\boldsymbol{\sigma}}^{(k)} = \boldsymbol{B}^{(k)}\bar{\boldsymbol{\sigma}}, \tag{8}$$

with $\boldsymbol{B}^{(k)}$ representing the stress concentration matrix of the subdomain $\Omega^{(k)}$.

The effective stiffness matrix of the homogenized masonry ($\boldsymbol{C}^*$) relates the macroscopic average stress to the average strain in the form

$$\bar{\boldsymbol{\sigma}} = \boldsymbol{C}^*\bar{\boldsymbol{\varepsilon}}. \tag{9}$$

Using eqs. (5)-(7), the following expression is directly obtained from eq. (9):

$$\boldsymbol{C}^* = \sum_{k=1}^{N} c^{(k)}\, \boldsymbol{C}^{(k)}\boldsymbol{A}^{(k)}. \tag{10}$$

Then, for the computation of the effective stiffness matrix using eq. (10), the strain concentration matrices of all subdomains contained in the RUC domain must be previously evaluated. In the next section, the procedures for determining such strain concentration matrices are reported.

3 Computational homogenization for masonry using finite-volume theory

3.1 Displacement and strain local fields of a subvolume

In the three-dimensional version of the Cartesian finite-volume theory, the repeating unit cell is discretized into parallelepipedal subvolumes defined by the locations of their eight vertices. For the homogenization approach, each fluctuating displacement component of the k-th subvolume is approximated by the polynomial expansion

$$\begin{aligned} u_i'^{(k)} = {} & W_{i(000)}^{(k)} + \bar{y}_1^{(k)} W_{i(100)}^{(k)} + \bar{y}_2^{(k)} W_{i(010)}^{(k)} + \bar{y}_3^{(k)} W_{i(001)}^{(k)} + \frac{1}{2}\left(3\bar{y}_1^{(k)2} + \frac{d_k^2}{4}\right) W_{i(200)}^{(k)} \\ & + \frac{1}{2}\left(3\bar{y}_2^{(k)2} + \frac{h_k^2}{4}\right) W_{i(020)}^{(k)} + \frac{1}{2}\left(3\bar{y}_3^{(k)2} + \frac{l_k^2}{4}\right) W_{i(002)}^{(k)}, \end{aligned} \tag{11}$$

where $\bar{y}_i$ indicates the subvolume local coordinates (see Fig. 2) and $W_{i(\cdots)}^{(k)}$ $(i = 1,2,3)$ are unknown coefficients to be determined. The local coordinate system $(\bar{y}_1, \bar{y}_2, \bar{y}_3)$ is centered in the subvolume. Here, d_k, h_k and l_k represent the side dimensions of the k-th subvolume in the directions 1, 2 and 3, respectively.

The strain components in the k-th subvolume are defined as

$$\varepsilon_{ij}^{(k)} = \bar{\varepsilon}_{ij} + \frac{1}{2}\left(\frac{\partial u_i'^{(k)}}{\partial \bar{y}_j} + \frac{\partial u_j'^{(k)}}{\partial \bar{y}_i}\right), \tag{12}$$

where $\bar{\varepsilon}_{ij}$ represents the components of the average strain $\bar{\boldsymbol{\varepsilon}}$ on the RUC domain.

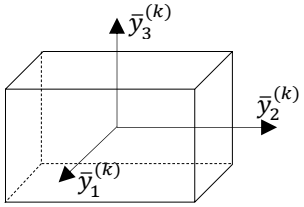

Figure 2. k-th subvolume and its local coordinate axes.

3.2 Local stiffness matrix of a subvolume

The surface-averaged fluctuating displacements on the k-th subvolume faces $(1,2,\cdots 6)$ are defined by

$$\bar{u}'^{(k)1,2}_i = \frac{1}{h_k l_k}\int_{-\frac{h_k}{2}}^{\frac{h_k}{2}}\int_{-\frac{l_k}{2}}^{\frac{l_k}{2}} u'^{(k)}_i\left(\pm\frac{d_k}{2},\bar{y}_2^{(k)},\bar{y}_3^{(k)}\right)d\bar{y}_2^{(k)}d\bar{y}_3^{(k)},$$

$$\bar{u}'^{(k)3,4}_i = \frac{1}{d_k l_k}\int_{-\frac{d_k}{2}}^{\frac{d_k}{2}}\int_{-\frac{l_k}{2}}^{\frac{l_k}{2}} u'^{(k)}_i\left(\bar{y}_1^{(k)},\pm\frac{h_k}{2},\bar{y}_3^{(k)}\right)d\bar{y}_1^{(k)}d\bar{y}_3^{(k)} \tag{13}$$

and

$$\bar{u}'^{(k)5,6}_i = \frac{1}{d_k h_k}\int_{-\frac{d_k}{2}}^{\frac{d_k}{2}}\int_{-\frac{h_k}{2}}^{\frac{h_k}{2}} u'^{(k)}_i\left(\bar{y}_1^{(k)},\bar{y}_2^{(k)},\pm\frac{l_k}{2}\right)d\bar{y}_1^{(k)}d\bar{y}_2^{(k)}.$$

Similarly, the surface-averaged tractions on the subvolume faces are given by the following relations:

$$\bar{t}_i^{(k)1,2} = \frac{1}{h_k l_k}\int_{-\frac{h_k}{2}}^{\frac{h_k}{2}}\int_{-\frac{l_k}{2}}^{\frac{l_k}{2}} t_i^{\boldsymbol{n}(k)}\left(\pm\frac{d_k}{2},\bar{y}_2^{(k)},\bar{y}_3^{(k)}\right)d\bar{y}_2^{(k)}d\bar{y}_3^{(k)},$$

$$\bar{t}_i^{(k)3,4} = \frac{1}{d_k l_k}\int_{-\frac{d_k}{2}}^{\frac{d_k}{2}}\int_{-\frac{l_k}{2}}^{\frac{l_k}{2}} t_i^{\boldsymbol{n}(k)}\left(\bar{y}_1^{(k)},\pm\frac{h_k}{2},\bar{y}_3^{(k)}\right)d\bar{y}_1^{(k)}d\bar{y}_3^{(k)} \tag{14}$$

and

$$\bar{t}_i^{(k)5,6} = \frac{1}{d_k h_k}\int_{-\frac{d_k}{2}}^{\frac{d_k}{2}}\int_{-\frac{h_k}{2}}^{\frac{h_k}{2}} t_i^{\boldsymbol{n}(k)}\left(\bar{y}_1^{(k)},\bar{y}_2^{(k)},\pm\frac{l_k}{2}\right)d\bar{y}_1^{(k)}d\bar{y}_2^{(k)}.$$

where $t_i^{\boldsymbol{n}(k)} = \sigma_{ji}^{(k)} n_j^{(k)}$, with $\sigma_{ji}^{(k)}$ and $n_j^{(k)}$ denoting the components of the stress $\boldsymbol{\sigma}^{(k)}$ and outward unit vector $\boldsymbol{n}^{(k)}$ normal to the corresponding subvolume face, respectively. The equilibrium equation of the k-th subvolume can be written in terms of the surface-averaged tractions as

$$\int_{S^{(k)}} t_i^{\boldsymbol{n}(k)} dS^{(k)} = 0, \tag{15}$$

where $S^{(k)}$ represents the subvolume surface areas.

Using eqs. (11)-(15) together with the subvolume constitutive relation, the following relation is obtained:

$$\bar{\boldsymbol{t}}^{(k)} = \boldsymbol{K}^{(k)}\bar{\boldsymbol{u}}'^{(k)} + \boldsymbol{N}\boldsymbol{C}^{(k)}\bar{\boldsymbol{\varepsilon}}, \tag{16}$$

where $\boldsymbol{N}$ is a matrix defined by the components of the outward unit vectors normal to the subvolume faces.

3.3 Global stiffness of the unit cell

Assembly of the global stiffness matrix is carried out by applying traction and displacement continuity conditions at the common interfaces between adjacent subvolumes of the repeating unit cell. The traction continuity conditions are imposed by applying force balance equations, which are then expressed in terms of the surface-averaged interfacial displacements using the local stiffness matrix equations. The displacement continuity conditions are directly enforced by setting the interfacial surface-averaged displacements to common values. The resulting system of equations has the following form

$$\boldsymbol{K}^{G}\overline{\boldsymbol{U}}' = \Delta\boldsymbol{C}\bar{\boldsymbol{\varepsilon}}, \tag{17}$$

where $\boldsymbol{K}^{G}$ is the global stiffness matrix of the RUC, $\Delta\boldsymbol{C}$ represents a matrix comprised of the differences in the local stiffness matrices of adjacent subvolumes and $\overline{\boldsymbol{U}}'$ is the surface-averaged fluctuating displacement global vector.

3.4 Effective stiffness matrix of the homogenized masonry

Using eq. (7), the average strain in the k-th subvolume can be written in function of the RUC macroscopic strain $\bar{\boldsymbol{\varepsilon}}$ in the form

$$\bar{\boldsymbol{\varepsilon}}^{(k)} = \boldsymbol{A}^{(k)}\bar{\boldsymbol{\varepsilon}}. \tag{18}$$

The evaluation of the effective stiffness matrix of the masonry is obtained by eq. (10), which involves the unknown strain concentration matrices of all subvolumes used in the RUC discretization. Based on eq. (18), each column of $\boldsymbol{A}^{(k)}$ can be determined by applying one nonzero macroscopic strain component $\bar{\varepsilon}_{ij}$ at a time and solving eq. (17) to obtain the corresponding average strain components $\bar{\varepsilon}_{ij}^{(k)}$ of the k-th subvolume. Then, for the three-dimensional homogenization problem, the computation of the six columns of each subvolume strain concentration matrix requires the application of appropriate macroscopic strain vector six times [8].

The average stress in the RUC domain ($\overline{\boldsymbol{\sigma}}$) and the effective stiffness matrix of the masonry ($\boldsymbol{C}^{*}$) can be obtained by the relations

$$\overline{\boldsymbol{\sigma}} = \frac{1}{DHL}\sum_{k=1}^{N_s} d_k h_k l_k\, \overline{\boldsymbol{\sigma}}^{(k)} \tag{19}$$

and

$$\boldsymbol{C}^{*} = \frac{1}{DHL}\sum_{k=1}^{N_s} d_k h_k l_k\, C^{(k)}\boldsymbol{A}^{(k)}, \tag{20}$$

where D, H and L are the RUC dimensions and N_s is the number of subvolumes.

4 Numerical results

For verification of the results provided by the three different FVDAM versions (PS, GPS and 3D-FVDAM), a periodic masonry made up of bricks and mortar joints arranged in running bond and stack bond patterns. The brick and mortar are assumed to be isotropic and linear elastic. The Young's moduli of the brick and mortar are $E_b = 2\times10^5\ MPa$ and $E_m = 2\times10^4 MPa$, respectively. It is assumed that brick and mortar present a same Poisson's ratio $\nu_b = \nu_m = 0.15$. The brick dimensions are $lenght = 0.21m$, $height = 0.05m$ and $width = 0.10m$. The joint mortar thickness is $0.01m$. For the analysis, the repeating unit cell has been discretized into subvolumes with $d_k = 10\ mm$, $h_k = 5\ mm$ and $l_k = 5\ mm$. Table 1 shows the effective elastic moduli for the running bond masonry, normalized by the corresponding brick elastic moduli, predicted by the PS, GPS and 3D-FVDAM formulations. For comparison, results obtained using finite-element method (FEM) [2] are also shown in Table 1. The effective elastic moduli for the stack bond masonry are shown in Table 2.

Tables 1 and 2 show that the effective elastic moduli obtained using GPS are the same provided by the 3D-FVDAM for four decimal places. It is also observed from Table 1 that the relative differences between the effective Young's moduli generated by the 3D-FVDAM and FEM model are smaller than 3.5%, whereas that for the effective shear moduli such relative differences are greater, reaching the value of 16.84% for G_{12}^{*}. These

differences can be justified by the way of applying the loading on the RUC surface. The macroscopic strain loading applied on the RUC surface is uniform in the FEM model, whereas it is periodic in the FVDAM formulation. Also, Tables 1 and 2 show that the greater difference between the corresponding effective elastic moduli predicted by the 3D-FVDAM for the cases of running bond and stacked bond is about of 7.35% and observed for G_{12}^{*}.

Table 1. Effective elastic moduli for the running bond masonry.

	E_{11}^{*}/E_b	E_{22}^{*}/E_b	E_{33}^{*}/E_b	G_{12}^{*}/G_b	G_{13}^{*}/G_b	G_{23}^{*}/G_b
PS	-	0.6517	0.3921	-	-	0.3663
GPS	0.8159	0.6549	0.3984	0.6778	0.3899	0.3666
3D	0.8159	0.6549	0.3984	0.6778	0.3899	0.3666
FEM [2]	0.8452	0.6786	0.4102	0.5801	0.3387	0.3311

Table 2. Effective elastic moduli for the stack bond masonry.

	E_{11}^{*}/E_b	E_{22}^{*}/E_b	E_{33}^{*}/E_b	G_{12}^{*}/G_b	G_{13}^{*}/G_b	G_{23}^{*}/G_b
PS	-	0.6402	0.4047	-	-	0.3602
GPS	0.8159	0.6291	0.4003	0.6280	0.3914	0.3602
3D	0.8159	0.6291	0.4003	0.6280	0.3914	0.3602

The average stresses on the RUC of the running bond pattern subjected to the macroscopic strain loading $\boldsymbol{\varepsilon}^{0} = (0, 0, -1, 0, 0, 0)$ are presented in Table 3. Due to the symmetry, the RUC average shear stresses are null. As can be seen, the values of the average stresses on the RUC predicted by the GPS and 3D formulations are very close.

Table 3. Average stresses on the RUC for the running bond pattern (Values in MPa).

	PS	GPS	3D	FEM [2]
σ_{11}^{*}	0.00	−14,189.20	−14,191.60	$-1.00E+04$
σ_{22}^{*}	−10,654.20	−12,815.70	−12,832.80	$-1.00E+04$
σ_{33}^{*}	−79,279.20	−81,778.70	−81,778.10	$-8.00E+04$

Table 3 shows that the average compressive stress components obtained using the PS condition are smaller than those provided by the GPS and 3D formulations. This indicates that the PS condition must be used with caution, for instance, in macroscopic failure analysis of masonry elements.

5 Conclusions

A study on the effective linear elastic response of periodic masonry constituted by bricks and mortar joints has been reported. The analyses have been developed by the FVDAM theory considering plane stress state (PS), generalized plane strain state (GPS) and a general 3D Cartesian formulation. Based on the results, the following main findings are briefly reported below:

1) In the linear elastic range, both the GPS and 3D assumptions produce close results.
2) For each brick arrangement (running bond or stack bond), the effective elastic moduli predicted by the GPS version and 3D formulation are very close.
3) The average stresses on the entire RUC obtained by the GPS version are not much different from those predicted by the 3D formulation.
4) The average stresses resulting from the PS condition present differences in relation to those generated by the other assumptions that can be relevant in nonlinear analyses (for instance, elastoplastic and damage).

Acknowledgements. The second author acknowledges the support provided by the Brazilian National Council for Scientific and Technological Development – CNPq to develop this work.

Authorship statement. The authors hereby confirm that they are the sole liable persons responsible for the authorship of this work, and that all material that has been herein included as part of the present paper is either the property (and authorship) of the authors, or has the permission of the owners to be included here.

References

[1] A. Zucchini, P. B. Lourenço, "A micro-mechanical model for the homogenisation of masonry". *International Journal of Solids and Structures*, vol. 39, pp. 3233–3255, 2002.
[2] N. Kumar, H. Lambadi, M. Pandey, A. Rajagopal, "Homogenization of Periodic Masonry Using Self-Consistent Scheme and Finite Element Method". *International Journal for Computational Methods in Engineering Science and Mechanics*, vol. 17, pp. 7–21, 2016.
[3] G. Wang, S. Li, H. -N. Nguyen, N. Sitar, "Effective Elastic Stiffness for Periodic Masonry Structures via Eigenstrain Homogenization". *Journal of Materials in Civil Engineering*, vol. 19, n. 3, pp. 269 – 277, 2007.
[4] Y. Zhou, L. J. Sluys, R. Esposito, "An improved mean-field homogenization model for the three-dimensional elastic properties of masonry". *European Journal of Mechanics/A Solids*, vol. 96, 10472, 2022.
[5] A. Anthoine, "Homogenization of periodic masonry: plane stress, generalized plane strain or 3d modelling". *Communications in Numerical Methods in Engineering*, vol. 13, 319–326, 1997.
[6] R. S. Escarpini Filho, F. P. A. Almeida, "Reinforced masonry homogenization by the finite-volume direct averaging micromechanics - FVDAM". *Composite Structures*, vol. 320, n. 15, 117185, 2023.
[7] F. P. A. Almeida, P. B. Lourenço, "Three-dimensional elastic properties of masonry by mechanics of structure gene". *International Journal of Solids and Structures*, vol. 191-192, 202–211, 2020.
[8] M. Gattu, H. Khatam, A. S. Drago, M. -J. Pindera, "Parametric finite-volume micromechanics of uniaxial continuously-reinforced periodic materials with elastic phases". *Journal of Engineering Materials and Technology*, vol. 130, 031015-1, 2008.